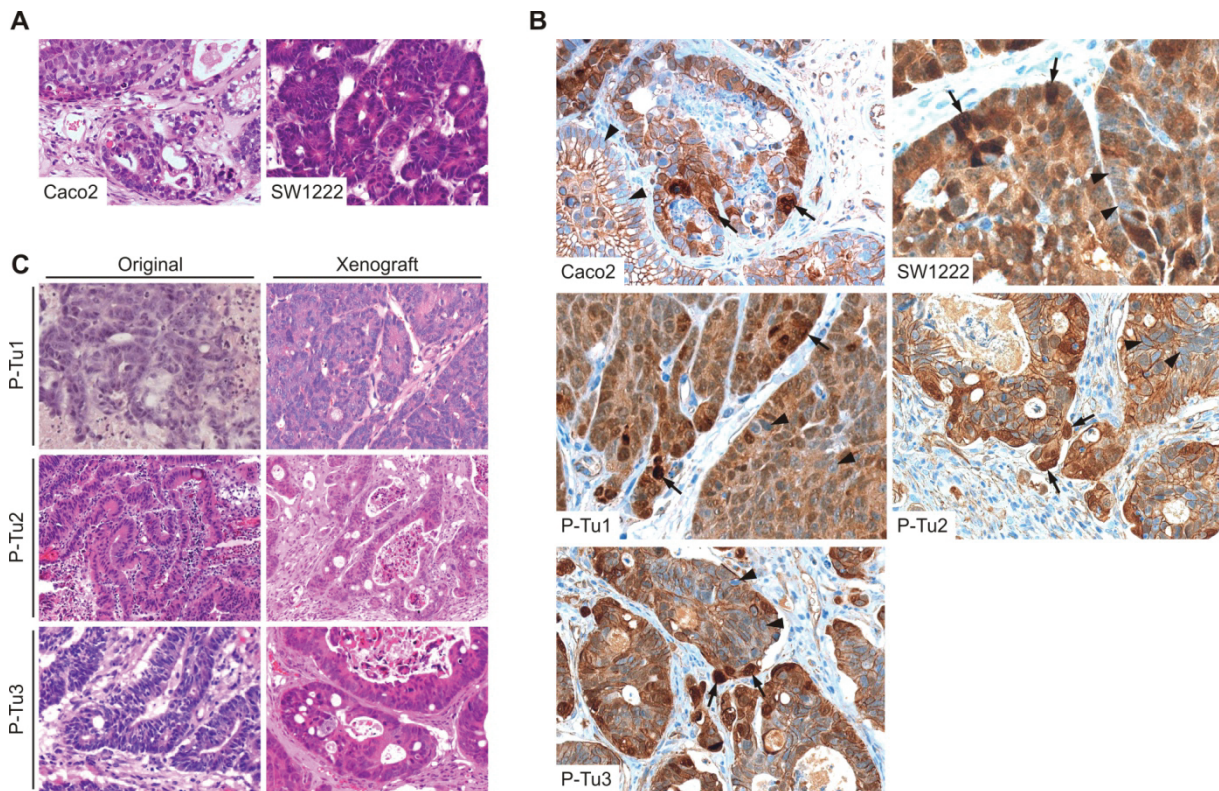
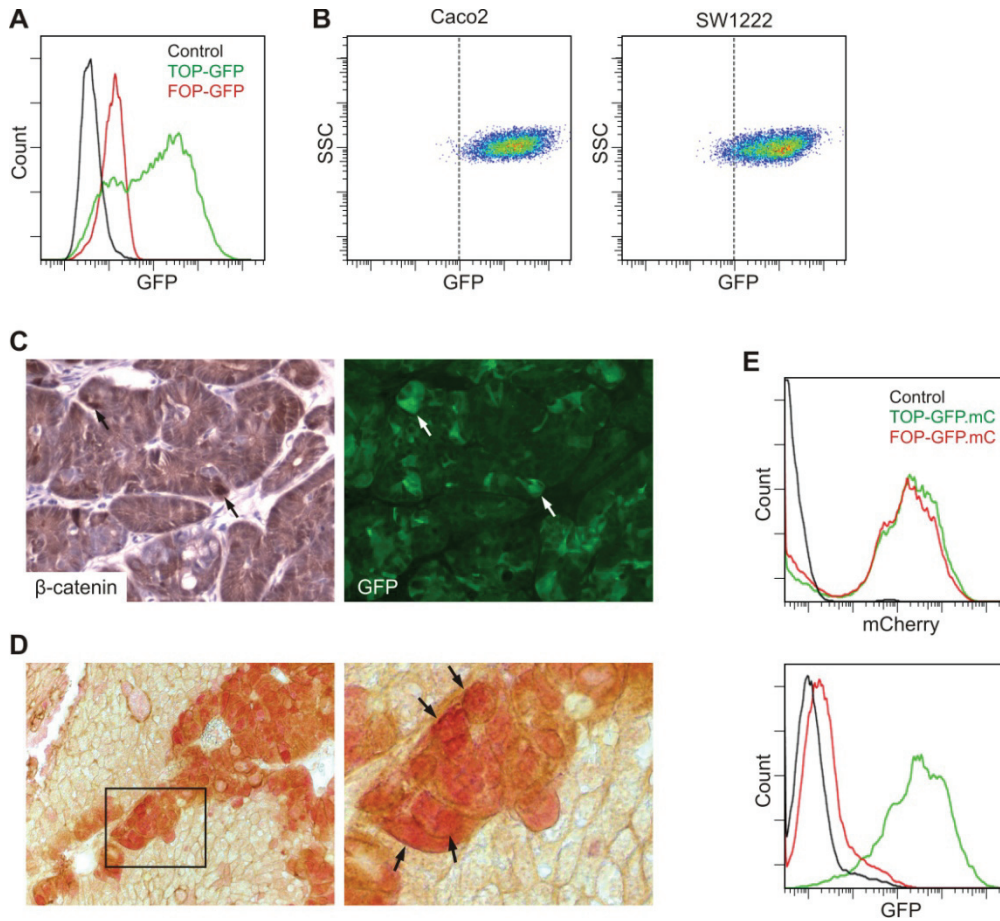


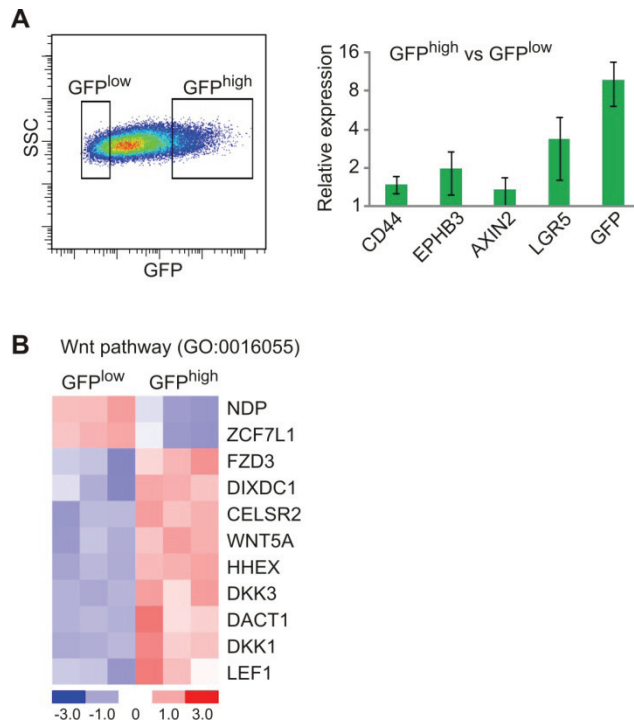
## SUPPLEMENTAL INFORMATION



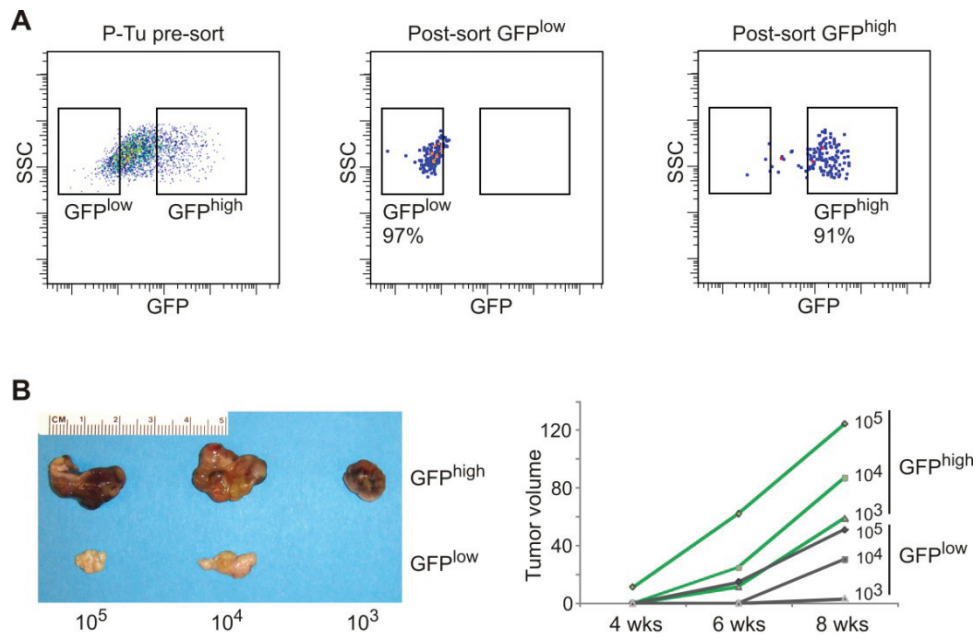
**Supplemental Figure 1.** (A) Hematoxylin and eosin (H&E)-stained sections of Caco2 (*left*) and SW1222 (*right*) CRC xenografts, showing adenocarcinoma morphology. (B)  $\beta$ -catenin immunostaining of all xenograft tumor sources used in this study showed strong nuclear accumulation in a subset of tumor cells (arrows), with the majority of cells showing little or no nuclear staining (arrowheads). (C) H&E staining demonstrates preserved glandular morphology of the original freshly resected colon cancer specimens (*left*, frozen sections) after xenografting and growth in NOD/SCID mice (*right*, paraffin sections).



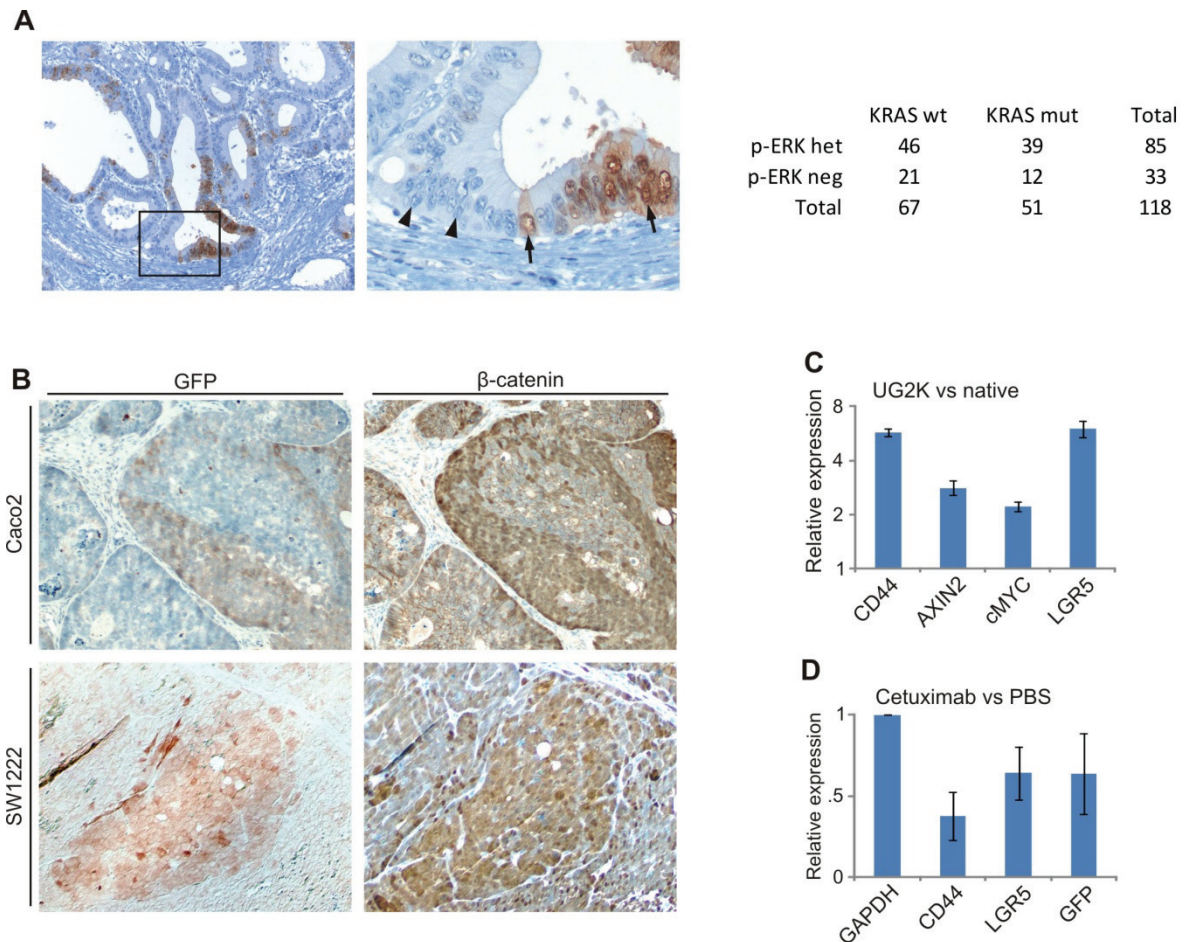
**Supplemental Figure 2.** (A) Specificity of TCF/LEF promoter-based GFP expression from the single color construct TOP-GFP in transduced Caco2 cells. Comparison of GFP fluorescence between non-transduced (Control), TOP-GFP, and FOP-GFP transduced Caco2 cells. (B) FACS analysis of *in vitro* cultured TOP-GFP transduced and single cell cloned Caco2 and SW1222 cells showing predominantly high GFP expression. (C) SW1222<sup>TOP-GFP</sup> xenograft tumor section, stained for  $\beta$ -catenin (*left*) and GFP (*right*) to assess co-localization (arrows) of the 2 proteins. (D) Co-immunostaining for active, dephospho- $\beta$ -Catenin (brown signal) and GFP (red signal) in Caco2<sup>TOP-GFP</sup> tumors reveals co-localization (arrows) of the two signals. *Right image* shows a higher magnification of area boxed in *left image*. (E) Specificity of TCF/LEF promoter-based GFP expression from the two-color construct TOP-GFP.mC. TCF/LEF promoter-independent mCherry fluorescence is present in both TOP-GFP.mC and FOP-GFP.mC transduced Caco2 cells (*top panel*), whereas TCF/LEF promoter-dependent GFP fluorescence is present only after TOP-GFP.mC transduction (*bottom panel*).



**Supplemental Figure 3.** (A) Flow sorting of disaggregated tumor cell suspensions from SW1222<sup>TOP-GFP</sup> xenografts (*left*) and qRT-PCR expression analysis of a panel of WNT-target genes (*right*). (B) Differentially expressed WNT pathway components in GFP<sup>high</sup> and GFP<sup>low</sup> tumor cells isolated from Caco2<sup>TOP-GFP</sup> xenografts.



**Supplemental Figure 4.** (A) Purity analyses of FACS sorted tumor cell fractions. *Left panel* shows GFP-fluorescence and gates during sort of a primary tumor (P-Tu). Purities (indicated as percent values) were assessed by immediate post-sort FACS analyses of GFP<sup>low</sup> (*middle panel*) and GFP<sup>high</sup> (*right panel*) cell fractions. (B) Gross appearance of tumors formed in NOD/SCID mice after 8 weeks (*left image*) and volume of tumors formed after 4-8 weeks (wks, *right graph*), following injection of the stated numbers of GFP<sup>high</sup> or GFP<sup>low</sup> cells isolated from Caco2<sup>TOP-GFP</sup> xenografts.



**Suppl. Figure 5.** (A) Immune staining for phospho-ERK in 118 colon cancer specimens reveals heterogeneous MAPK activity, irrespective of KRAS mutation status. In all tumors with detectable phospho-ERK staining, tumor cells with (*arrows*) and without (*arrowheads*) staining were present. *Right image* shows a higher magnification of area boxed in *left image*. *Table* indicates frequencies of non-detectable (*p-ERK neg*) and heterogeneous ERK expression (*p-ERK het*) in colon cancers with (*KRAS mut*) and without (*KRAS wt*) KRAS mutations. (B) Serial sections of mosaic Caco2<sup>UG2K</sup> and SW1222<sup>UG2K</sup> transduced tumors, stained for  $\beta$ -catenin and GFP, showing co-localization of GFP (and hence KRAS<sup>G12V</sup>) expression and nuclear  $\beta$ -catenin. (C) qRT-PCR analysis of expression of a panel of WNT target genes in UG2K transduced Caco2 tumor cells, normalized to non-transduced (native) cells, providing evidence for WNT pathway activation. (D) Cultured Caco2<sup>TOP-GFP</sup> cells were treated with cetuximab or PBS for 5 days. qRT-PCR analysis showed decreased expression of GFP and of the WNT target genes CD44 and LGR5.

**Suppl. Table 1. Gene Expression (real-time RT-PCR) primers used in this study**

Primers were selected from the Universal Probe Library (Roche). TCF1 primers were previously described (Maier et al., 2011).

<b>Gene</b>	<b>Forward Primer</b>	<b>Reverse Primer</b>
AXIN2	aggccagtgagttggttgc	catcctcccagatctctca
BMP4	ctttaccggcttcagtctgg	tgggatgttctccagatgttc
CD44	aaggtggagcaaacacaacc	tccacttggtttctgtcct
cMYC	cctaccctctcaacgacagc	ctctgacctttgccaggag
DKK1	caggcgtgcaaactctgtct	aatgattttgatcagaagacacacata
EPHB3	cagaagacctgctccgtattgg	tcacccctctcctaattccatc
GAPDH	gaaggtgaaggtcggagtc	gaagatggtgatgggatttc
GFP	agaacggcatcaaggtgaac	tgctcaggtagtggttgcg
LGR5	ggaaatcatgccttacagagc	cctggggaaggtgaacact
mCherry	ccccgtaatgcagaagaaga	ttgacctcagcgtcgtagtg
NKD1	gctgctgggtaaagctcac	agtgggcttggctctctgct
SP5	gaagctcaaagtcgctgagg	caggtccccggatctctc
TCF1	cgggacagaggaccattacaactagatcaaggag	ccacctgcctcggcctgccaagt

**Supplemental Reference**

Maier E, Hebenstreit D, Posselt G, Hammerl P, Duschl A, Horejs-Hoeck J. Inhibition of suppressive T cell factor 1 (TCF-1) isoforms in naive CD4+ T cells is mediated by IL-4/STAT6 signaling. *The Journal of biological chemistry* (2011) 286:919-928.